72215

Aphanitic Impact Melt Breccia
St. 2, 379.2 g

INTRODUCTION

72215 is an aphanitic, clast-rich impact melt that the crew sampled as a rounded clast in Boulder 1 (see section on Boulder 1, St. 2, Fig. 2). Its groundmass crystallized about 3.83 Ga ago. The sample, which is nearly 10 cm long, is irregularly shaped (Fig. 1), tough, and medium light gray [N5-N6]. The exposed surface had many zap pits with glass linings.

72215 proved to be the most coherent of the four samples collected from Boulder 1. It is a fine-grained, foliated and heterogeneous, medium gray polymict breccia. A few of the clasts in 72215 are more than a centimeter across (Fig. 1). The clast population comprises a wide variety of lithic and mineral types. The bulk rock has a low-K Fra Mauro composition that is a little more aluminous and a little less titaniferous than the coarser poikilitic Apollo 17 impact melt rocks. Laser Ar-Ar ages show an age of about 3.83 Ga for the crystallization of the groundmass. Sr isotopes did not equilibrate between melt and even tiny clasts, showing that the high temperature period was very short. Rare gas analyses suggest an exposure age of about 42 Ma.

Most of the studies of 72215 were conducted by the Consortium Indomitable (leader J.A. Wood). A slab cut lengthwise across the foliation of 72215 (Fig. 2) made a comprehensive petrographic and chemical study possible. Detailed maps of the exterior surfaces and the slab based on the macroscopic observations, as well as descriptions of the sample allocations, were given in Stoeser et al. (in Cl 2, 1974).

PETROGRAPHY

Specimen 72215 consists of coherent material, with a rounded knob encrusted with a poikilitic anorthositic breccia at one end (Marvin, 1975; CI 2, 1974). LSPET (1973) described the sample as a layered light gray

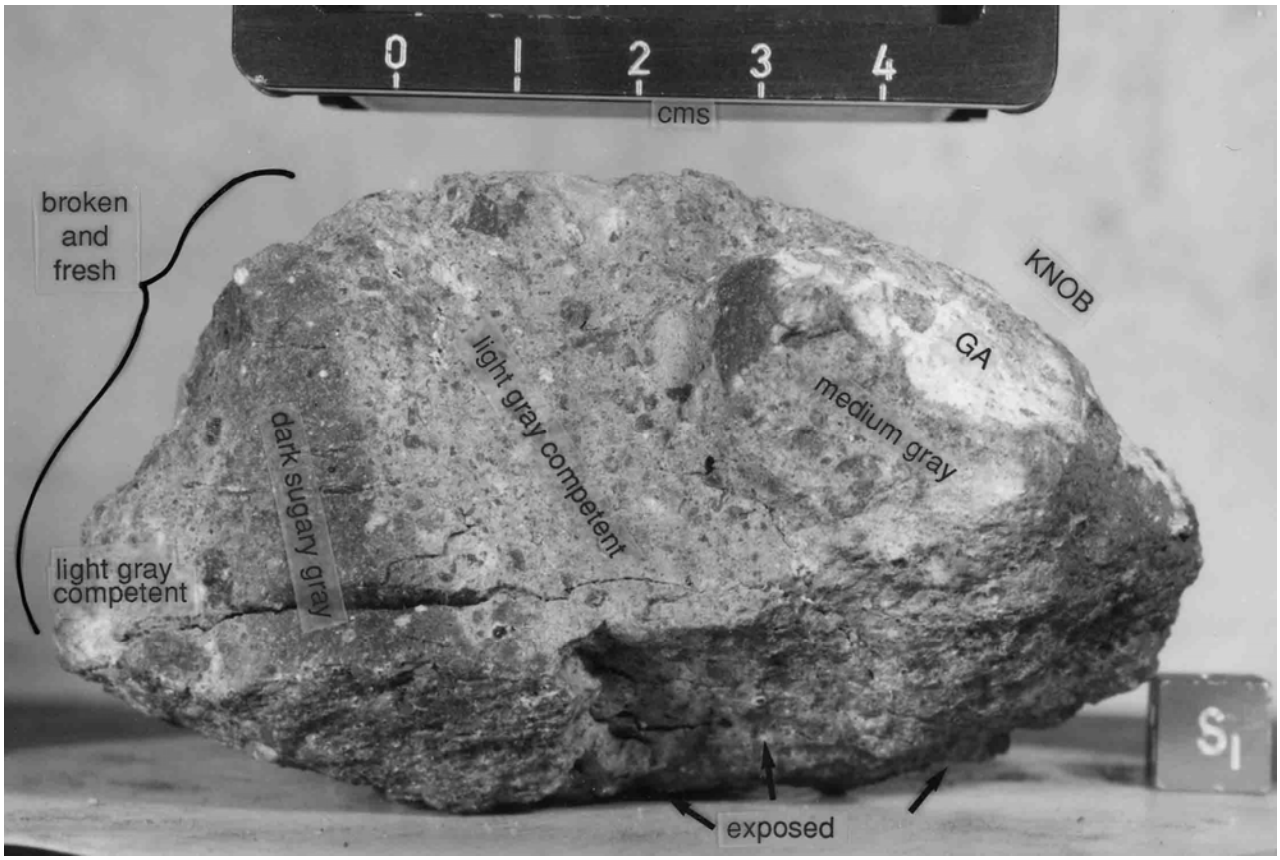

Figure 1: South (arbitrary) face of 72215 prior to slabbing. Most of the upper part visible is the freshly broken surface; the lower part visible was exposed and shows patina and zap pits. S-73-23563.

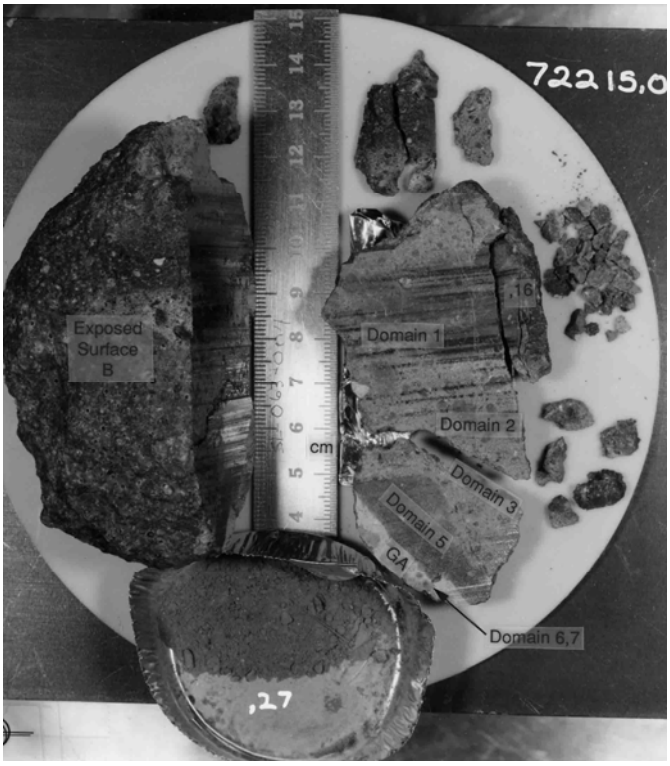

Figure 2: Slab cut from 72215 in 1974. The slab was further subdivided. S-74-21189.

breccia; Simonds et al. (1975) listed it as a fragmental breccia (clast-supported); and Stoffler et al. (1979) and Knoll et al. (1979) included it among their granular crystalline matrix breccias, a product of crystallization of a fragment-laden melt. The most detailed descriptions of the petrography of 72215 are given in Stoeser et al. (in CI 2, 1974) and in Ryder et al. (1975), although these refer to the sample as metamorphic rather than impact melt (nonetheless noting the obvious shearing, areas of melting, and fluidity of the sample during the high-temperature phase). That the groundmass texture is that of a melt was recognized later (e.g. James, 1977; Stoffler et al., 1979).

The main mass consists of gray breccia that ranges in color from light chalky to dark sugary gray (Figs. 1, 2). The darker material, which is more coherent and uniform than the rest, appears as an irregular band through the matrix, and as a partial rim on the knob. In thin sections the colors and textures are virtually indistinguishable. Typical matrix is shown in Fig. 3a. It consists of angular to rounded mineral and lithic clasts with a seriate grain-size down to about 20 microns. The host melt material is very fine-grained with pyroxenes and plagioclases less than a few microns across; Simonds et al. (1975) quoted less than 5 microns for both phases in the groundmass. In some places the clasts include obvious dark blobs of essentially similar material (Fig. 3b).

Stoeser et al. (in C12, 1974), on the basis of macroscopic observations and a set of thin sections from the slab that traversed the entire sample, subdivided 72215 into seven domains (Fig. 4). Four domains are melt matrix (referred to by Stoeser et al. as dark matrix breccias) and three are cataclastic poikilitic poikiloblastic feldspathic granulites (referred to by Stoeser et al. as cataclastic granulitic and poikilitic ANT breccias). The latter are essentially large crushed clasts. Most of the sample consists of the melt matrix material.

Domains 1-3: Domains 1 and 2 were distinguished because of megascopic differences, with 1 corresponding with dark sugary gray material and 2 corresponding with light sugary gray material. Domain 3 was distinguished from 2 only because of a hiatus in the sampling. All three are very similar in thin sections, consisting of dark melt breccias with a variety of clasts including globby dark clasts of material similar to the matrix itself. The darkest globs are vesicular. In domain 3 the material to the left of the dashed line (Fig. 4) is denser, darker, and more vesicular than that to the right. Defocused beam microprobe analyses of the matrix domains show that all three are very similar in composition (Table 1).

Domain 5: Domain 5 is darker than the others, and has a more vesicular groundmass. In some thin sections it appears to be continuous with the denser portion of domain 3. It is distinct from the other melt domains in its greater abundance of granitic clasts (Table 2). The defocused beam analyses show that the bulk composition of domain 5 is also distinct in being far more potassic (Table 1). Silicate mineral analyses for domain 5 (Fig. 5) show populations similar to those of other Boulder 1 melt matrices.

Domains 4 and 7, Cataclastic feldspathic granulite: (cataclastic granulitic ANT breccia of Stoeser et al., in CI 2, 1974; and Ryder et al., 1975). Domain 4 consists of brecciated material that is crushed, fine-grained feldspathic granulite, strung out into a lenticular mass (Fig. 4), and mixed to some degree into domains 3 and 5. Following cataclasis, annealing was sufficient to eliminate porosity. The feldspathic granulite is finer-grained and more heterogeneous than the poikilitic variety in domain 6. A

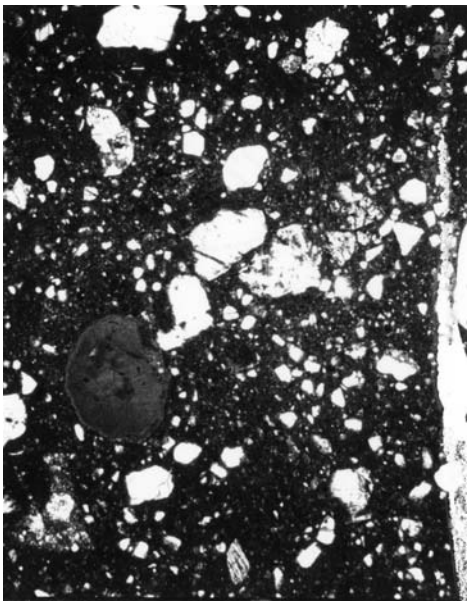

a

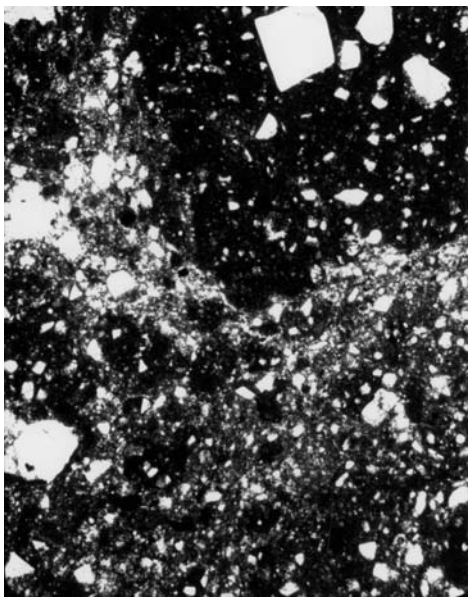

b

c

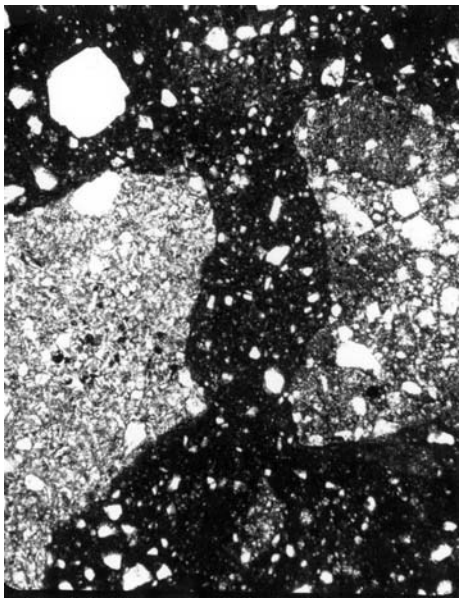

d

Figure 3: Photomicrographs of 72215. All plane transmitted light, all about 1 mm width of view.
a) 72215,184, typical dense dark groundmass, showing fine grain size of matrix and abundance of small clasts.
b) 72215,193, blobby groundmass in Domain 1.
c) 72215,107, poikilitic feldspathic granulite (lithology GA) and crushed equivalent that is Domain 6.
d) 72215,184, basaltic-textured melt clast (left) and feldspathic breccia (right) in Domain 2 groundmass.

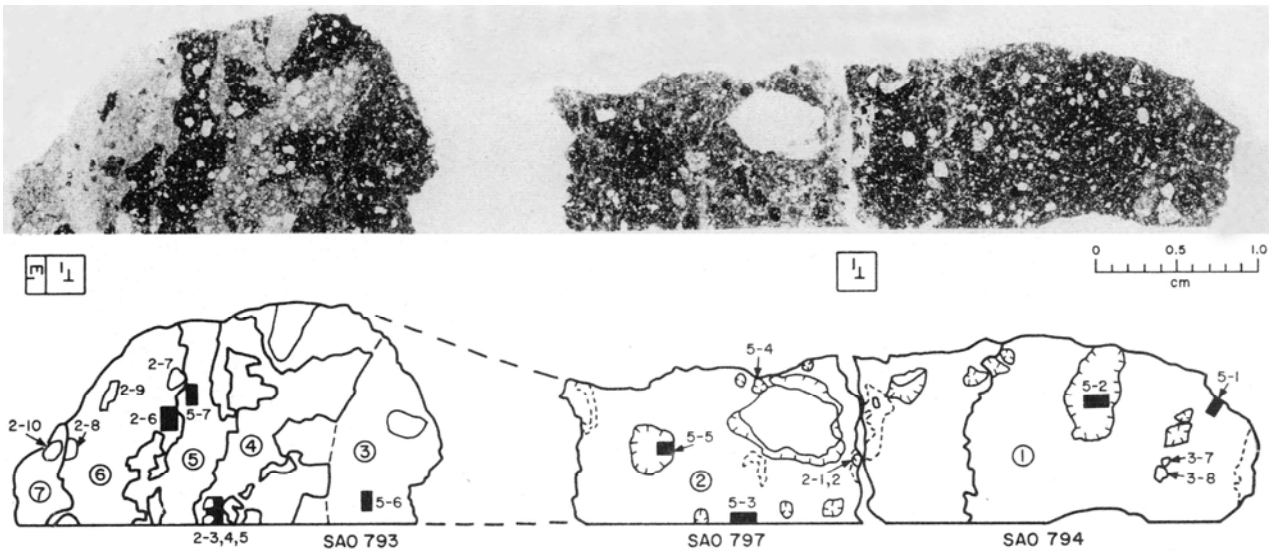

Figure 4: Photographs and sketch maps of traverse through 72215 (from Stoeser et al., in C12, 1974), showing domain designations as circled numbers. The knob is to the left.

defocused beam microprobe analysis (Table 1) shows that it is also less feldspathic than domain 6, with a lower mg'. The domain 7 granulite is very similar to that of domain 4, and has a sharp contact with domain 6.

Domain 6, Cataclastic poikilitic feldspathic granulite: (cataclastic poikilitic ANT breccia of Stoeser et al., in CI 2,1974; also Clast 4). Domain 6 consists mainly of a cataclasized, coarse-grained, poikilitic granulite 3 (Fig. 3c). Equi-dimensional chadacrysts of plagioclase (An90.96) are embedded in pyroxene oikocrysts (En74-77W03-5) that are more than 4 mm across. Augite and olivine are present but minor. Some of the plagioclases contain small spherical inclusions of mafic minerals. Modally the granulite is an anorthositic norite, as also shown by the microprobe defocused beam analysis (Table 1). Domain 6 also contains some minor clear brown and finely devitrified glass and finer granulitic material.

Goldstein *et al.* (1976a,b) analyzed metal and cohenite (Fe,Ni)3C in 72215 melt (from domain 2). They found an equant bleb of kamacite that contained both carbide (cohenite) and residual taenite. The Ni content of the taenite is higher than that in the metal of iron meteorites; the Ni at the alpha/ gamma interface indicates equilibration down to about 500 degrees C.

Stoeser *et al*. (in Cl 2, 1974) tabulated a survey of clast populations in the melt domains (Table 2). The populations of each are similar, except that domain 5, which is comparatively darker and more vesicular, has a much higher proportion of granitic clasts. The populations (clasts larger than 0.2 mm) are dominated by feldspathic granulites (~20%), anorthositic breccias (~8%), and plagioclase (including devitrified maskelynite) fragments (~2540%). Stoeser et al. (1974, in CI 2) reported bulk analyses by microprobe defocused beam for several of these clasts (Table lb); they show a range of compositions with mg' varying from 0.63 to 0.80. Other lithic fragments include various basaltic-textured ones (~2%), granites (4-23%), ultramafics, and norites (less than 2%). Other mineral clasts include pyroxene, olivine, spinels, and silica phases. Examples of the anorthositic breccia and a basaltic-textured fragment are shown in Fig. 3d. The latter, some of which contain small pink spinels, are probably at least mainly impact melts. Defocused beam analyses show that they are aluminous, olivine-normative fragments (Table 1c).

The granitic clasts in Boulder 1, including those in 72215, were described by Stoeser et al. (1975) and Ryder *et Al* (1975), with photomicrographs of some clasts. Those in 72215 show the range of petrographic features typical of those elsewhere in the Boulder. They are characterized by their high K2O (6-10%) and SiO2 (70-80%) as shown by defocused beam analyses. Some clasts are glassy, others crystalline, the latter consisting mainly of potash feldspar, silica, plagioclase feldspar, and pyroxenes. Some of those in 72215 show feldspars in the forbidden region of the compositional field (ternary feldspars) (Fig. 6a). Pyroxenes are iron-rich augites and pigeonites.

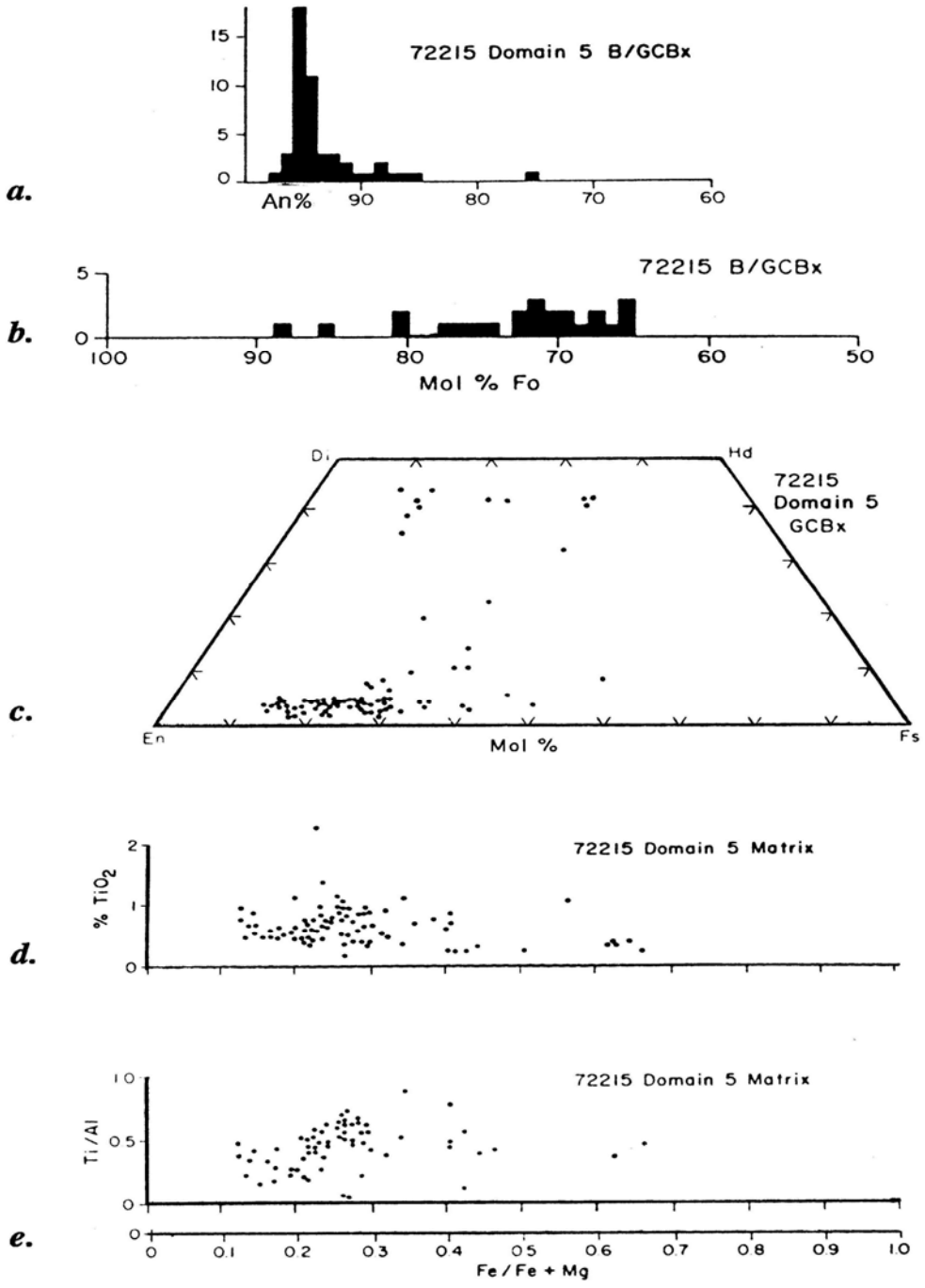

Figure 5: Compositions of plagioclases (a), olivines (b), and pyroxenes (c,d,e) in domain 5 (from Ryder et al., 1975). Most of these analyses are for mineral clasts, rather than for the tiny melt-crystallized phases.

Table 1: Defocused beam analyses of materials in 72215
(from Stoeser *et al*., in CI 2, 1974).

a) melt matrices (dark matrix breccias).

	1.	2.	3.	4.	5.	6.	7.
	794	794C10	797	797C4	797C6	793	793
	matrix dom. 1	vesic. DMB clast	matrix dom. 2	vesic. DMB clast	nonvesic. DMB clast	matrix dom. 3	matrix dom. 5
WT. % OXIDES							
SiO_2	46.20	48.04	45.05	45.52	46.78	46.75	48.02
TiO_2	0.56	0.79	0.60	0.60	0.58	0.68	0.66
Al_2O_3	18.30	16.86	19.81	17.38	18.31	19.64	18.79
Cr_2O_3	0.14	0.15	0.13	0.12	0.18	0.14	0.04
FeO	8.39	8.30	7.32	8.40	8.86	8.20	8.00
MnO	0.12	0.11	0.12	0.17	0.12	0.11	0.12
MgO	11.04	13.46	9.71	14.16	11.39	10.54	7.32
CaO	12.01	10.80	12.62	11.31	12.10	12.73	11.81
Na_2O	0.51	0.56	0.56	0.55	0.57	0.49	0.77
K_2O	0.21	0.29	0.18	0.21	0.25	0.22	1.02
BaO	0.03	0.04	0.09	0.14	0.11	0.05	0.09
P_2O_5	0.24	0.19	0.21	0.19	0.21	0.18	0.34
TOTAL	97.74	99.58	96.39	98.74	99.47	99.75	97.00
CIPW NORM							
FO	5.7	5.8	5.8	13.9	7.0	5.7	---
FA	3.3	2.7	3.3	6.4	4.2	3.3	---
EN	20.0	25.4	16.8	16.0	18.5	18.2	18.8
FS	10.6	10.6	8.7	6.6	10.0	9.7	14.2
WO	4.7	4.1	4.5	4.5	5.1	4.7	5.0
OR	1.3	1.7	1.1	1.3	1.5	1.3	6.2
AB	4.4	4.7	4.9	4.7	4.9	4.2	6.7
AN	48.1	42.8	53.0	44.9	47.0	50.9	46.2
ILM	1.1	1.5	1.2	1.2	1.1	1.3	1.3
CHR	0.2	0.2	0.2	0.2	0.3	0.2	0.1
QTZ	---	---	---	---	---	---	0.6
COR	---	---	---	---	---	---	---
AP	0.6	0.4	0.5	0.4	0.5	0.4	0.8
COMP. NORM MIN.							
OL: FO	71.2	75.9	71.7	76.0	70.8	71.1	---
PX: EN	62.1	68.6	61.5	64.1	60.6	61.3	55.4
FS	25.1	21.8	24.3	20.3	25.0	24.9	31.9
WO	12.7	9.6	14.2	15.6	14.3	13.7	12.8
PLAG: OR	2.3	3.4	1.8	2.4	2.7	2.3	10.4
AB	8.7	10.2	8.9	9.9	9.7	7.8	12.0
AN	89.0	86.4	89.3	87.7	87.6	89.9	77.6
atomic Mg/(Mg+Fe)	0.701	0.742	0.702	0.750	0.696	0.696	0.619
MgO/(MgO+FeO)	0.568	0.619	0.570	0.628	0.562	0.562	0.478
No. of analyses	14	15	21	11	14	16	15

b) feldspathic breccia ("ANT-suite") clasts.

	1.	2.	3.	4.	5.	6.	7.	8.	9.	10.
WT. % OXIDES	797C2A anorth. breccia clast	797C2B "glassy vein"	793 dom. 4 gran. ANT breccia	793C6 gran. ANT clast	793C7 gran. ANT clast	793 dom. 6 ANT breccia	793C2 poik. ANT clast	793C4 poik. ANT clast	793C1 glass vein in poik. ANT	793C3 gran. ANT clast
SiO_2	45.17	43.68	47.48	46.59	48.41	45.81	46.43	46.26	45.23	47.56
TiO_2	0.50	1.17	0.79	0.43	0.11	0.61	0.12	0.19	0.11	0.18
Al_2O_3	28.62	23.05	23.14	26.45	22.56	23.93	26.89	25.55	25.45	22.32
Cr_2O_3	0.05	0.05	0.04	0.51	0.07	0.07	0.07	0.10	0.06	0.04
FeO	2.05	5.17	6.63	4.93	7.08	5.83	3.47	4.15	4.19	6.83
MnO	0.06	0.11	0.05	0.07	0.08	0.05	0.06	0.10	0.09	0.15
MgO	2.73	11.48	6.37	5.12	8.17	7.09	6.97	7.76	7.65	7.77
CaO	16.17	13.72	14.76	15.37	13.46	14.72	15.15	14.40	15.49	13.32
Na_2O	1.00	0.74	0.58	0.65	0.64	0.46	0.44	0.38	0.50	0.69
K_2O	0.31	0.19	0.34	0.17	0.14	0.28	0.08	0.11	0.11	0.33
BaO	0.07	0.09	0.07	0.04	0.06	0.10	0.04	0.03	0.03	0.10
P_2O_5	0.03	0.06	0.66	0.27	0.60	0.39	0.01	n.d.	0.02	0.10
TOTAL	96.77	99.49	100.89	100.59	101.37	99.36	99.74	99.06	98.93	99.39
CPIW NORM										
FO	0.5	18.2	---	0.1	0.1	2.7	2.3	2.5	7.3	2.2
FA	0.2	5.4	---	---	0.1	1.7	0.9	1.0	3.2	1.6
EN	6.4	2.8	15.7	12.6	19.9	13.9	14.1	16.0	8.9	16.3
FS	2.8	0.8	10.8	7.9	12.6	7.7	5.1	6.1	3.6	10.5
WO	3.2	3.7	3.9	2.4	1.9	3.4	1.7	1.6	4.2	3.7
OR	1.9	1.1	2.0	1.0	0.8	1.7	0.5	0.7	0.7	2.0
AB	8.8	6.3	4.9	5.5	5.4	3.9	3.7	3.2	4.3	5.9
AN	75.1	59.4	59.0	68.4	57.5	62.9	71.4	68.3	67.6	57.2
ILM	1.0	2.2	1.5	0.8	0.2	1.2	0.2	0.4	0.2	0.3
CHR	0.1	0.1	0.1	0.7	0.1	0.1	0.1	0.1	0.1	0.1
QTZ	---	---	0.6	---	---	---	---	---	---	---
COR	---	---	---	---	---	---	---	---	---	---
AP	0.1	0.1	1.5	0.6	1.3	0.9	---	---	---	0.2
COMP. NORM. MIN.										
OL: FO	---	82.9	---	---	---	70.4	78.6	77.4	76.6	67.1
PX: EN	56.5	42.7	57.5	60.8	63.8	61.2	72.6	72.5	58.4	59.4
FS	19.0	8.8	30.1	29.1	30.9	25.9	19.8	21.2	17.8	29.2
WO	24.5	48.5	12.4	10.0	5.3	13.0	7.6	6.3	23.7	11.5
PLAG: OR	2.2	1.6	3.0	1.3	1.2	2.0	0.6	0.9	0.9	3.0
AB	10.7	10.0	7.8	7.7	9.0	6.5	5.2	4.7	6.2	9.6
AN	87.1	88.4	89.2	91.0	89.8	91.5	94.2	94.3	92.8	87.4
atomic Mg/(Mg+Fe)	0.704	0.798	0.631	0.650	0.672	0.683	0.781	0.769	0.765	0.670
MgO/(MgO+FeO)	0.571	0.689	0.490	0.509	0.536	0.548	0.667	0.651	0.646	0.532
No. of analyses	7	6	14	8	7	15	20	23	8	15

c) pink spinel troctolite basalts.

	794C1 PSTB	794C2 ol-pheno. basalt
WT. % OXIDES		
SiO_2	48.17	43.67
TiO_2	0.36	0.20
Al_2O_3	22.30	18.86
Cr_2O_3	0.05	0.04
FeO	4.73	6.73
MnO	0.07	0.07
MgO	9.07	17.24
CaO	14.44	11.31
Na_2O	0.51	0.39
K_2O	0.35	0.09
BaO	n.d.	n.d.
P_2O_5	0.06	0.09
TOTAL	100.11	98.71
CIPW NORM		
FO	2.2	25.1
FA	0.9	7.8
EN	19.5	7.7

FS		7.1	2.2
WO		5.7	2.6
OR		2.1	0.6
AB		4.3	3.3
AN		57.3	50.1
ILM		0.7	0.4
CHR		0.1	0.1
QTZ		---	---
COR		---	---
AP		0.1	0.2
COMP. NORM MIN.			
OL:	FO	78.4	82.3
PX:	EN	65.3	66.3
	FS	18.0	14.4
	WO	16.7	19.4
PLAG:	OR	3.2	1.0
	AB	7.1	6.6
	AN	89.7	92.4
atomic Mg/(Mg+Fe)		0.773	0.820
MgO/(MgO+FeO)		0.657	0.719
No. of analyses		12	12

Table 2: Clast populations of 72215 matrices; percentages by volume, in three size categories
(from Stoeser *et aL*, in CI 2, 1974).

	DOMAINS 1 + 2				DOMAIN 3				DOMAIN 5			
	0.2-0.5 mm	0.5-1.0 mm	>1.0 mm	TOTALS	0.2-0.5 mm	0.5-1.0 mm	>1.0 mm	TOTALS	0.2-0.5 mm	0.5-1.0 mm	>1.0 mm	TOTALS
ANT suite	(26.1)	(5.5)	(3.7)	(35.3)	(32.6)	(7.7)	(1.5)	(41.8)	(31.9)	(4.3)	(2.6)	(38.8)
ANT breccias	(4.4)	(1.8)	(2.0)	(8.2)	(5.7)	(0.5)	(0.5)	(6.7)	(7.8)	-	-	(7.8)
mafic	0.6	0.2	0.2	1.0	-	-	-	-	-	-	-	-
gabbroic	2.1	1.1	1.2	4.4	4.3	0.5	0.5	5.3	7.8	-	-	7.8
anorthositic	1.7	0.5	0.6	2.8	1.4	-	-	1.4	-	-	-	-
Granulitic ANT	(15.5)	(2.3)	(1.0)	(19.8)	(16.3)	(6.2)	(1.0)	(23.5)	(18.1)	(4.3)	(2.6)	(25.0)
gabbroic	13.6	2.3	0.8	16.7	13.9	6.2	1.0	21.1	16.4	4.3	2.6	23.3
anorthositic	2.9	-	0.2	3.1	2.4	-	-	2.4	1.7	-	-	1.7
Poikiloblastic ANT	0.6	0.3	-	0.9	1.0	-	-	1.0	-	-	-	-
Poikilitic ANT	0.9	0.2	0.2	1.3	5.3	-	-	5.3	2.6	-	-	2.6
Coarse ANT	3.1	0.9	0.5	4.5	4.3	1.0	-	5.3	3.4	-	-	3.4
Unclassified ANT	0.6	-	-	0.6	-	-	-	-	-	-	-	-
Ultramafic particles	2.0	0.2	0.2	2.4	1.4	-	-	1.4	1.7	-	-	1.7
Basalts	(1.6)	(1.1)	(0.9)	(3.6)	(1.4)	-	-	(1.4)	(0.9)	-	-	(0.9)
Ol.-norm. pig. bas.	-	0.3	0.5	0.8	-	-	-	-	-	-	-	-
pink sp. troct. bas.	0.9	0.6	0.2	1.7	1.4	-	-	1.4	0.9	-	-	0.9
mafic troct. bas.	0.2	-	-	0.2	-	-	-	-	-	-	-	-
unclassified bas.	0.5	0.2	0.2	0.9	-	-	-	-	-	-	-	-
Microgranites	3.4	0.6	0.2	4.2	8.6	2.4	-	11.0	19.8	3.4	-	23.2
Civet Cat norite	-	-	0.2	0.2	0.5	-	-	0.5	-	-	-	-
Devitrified maskelynite	12.0	1.7	0.3	14.0	8.6	1.4	-	10.0	2.6	-	-	2.6
Glassy clasts	0.2	0.2	-	0.4	-	-	-	-	-	-	-	-
Mineral fragments	(38.3)	(2.1)	-	(40.4)	(31.5)	(2.5)	-	(34.0)	(30.2)	(2.6)	-	(32.8)
Plagioclase	23.4	1.1	-	24.3	16.7	1.0	-	17.7	19.0	2.6	-	21.6
Olivine	4.9	0.2	-	5.1	6.2	0.5	-	6.7	1.7	-	-	1.7
Pyroxene	9.8	0.8	-	10.6	8.1	1.0	-	9.1	9.5	-	-	9.5
Chromite	0.2	-	-	0.2	-	-	-	-	-	-	-	-
Silica phases	-	-	-	-	0.5	-	-	0.5	-	-	-	-
TOTAL %	83.6	11.4	5.5	100.5	84.6	13.0	1.5	100.1	87.1	10.3	2.6	100.0
NO. OF CLASTS	547	72	33	652	177	29	3	209	101	12	3	116

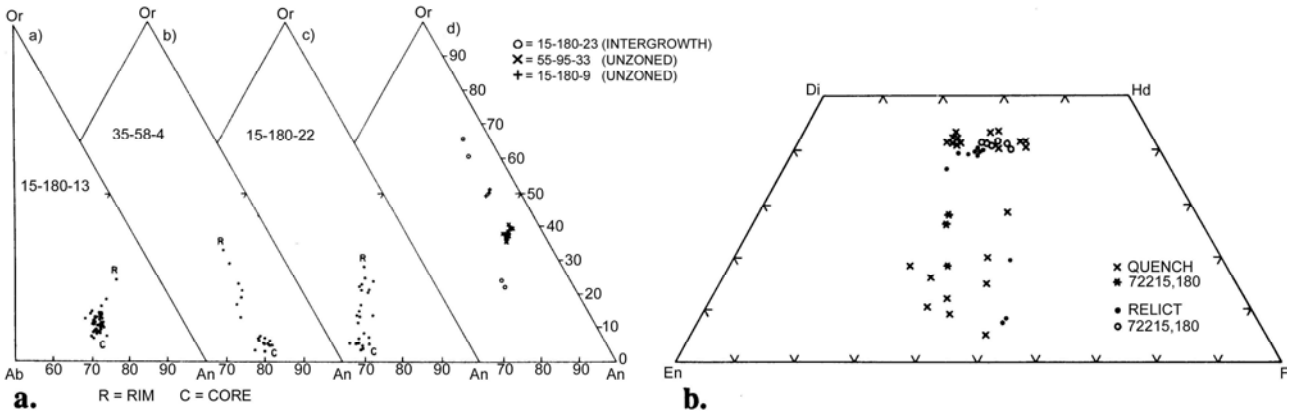

Figure 6: Compositions of minerals in granitic fragments from 72215 and other Boulder 1 samples. a) Plagioclase feldspars. b) Pyroxenes, Ryder et al., 1975.

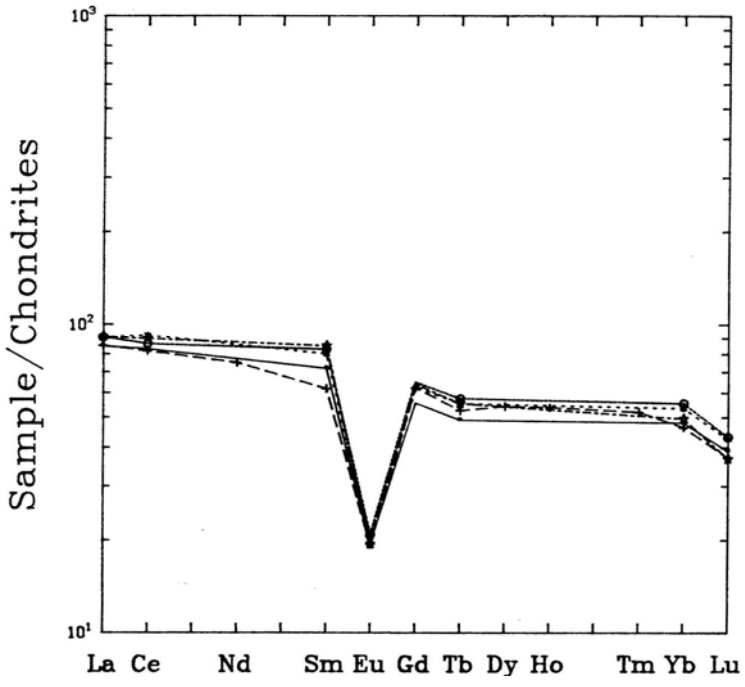

Figure 7: Rare earth element plots of matrices/bulk rock samples of 72215. Solid line and dots =, 64; spaced dotted line =, 60, close dotted line with open circles =,47; dot-dash line =,92; all Blanchard et al. (1975). Dashed line and crosses =, 22; Palme et al. (1978).

Spudis and Ryder (1981) showed photomicrographs of clasts in 72215, including granoblastic ones and clasts with accretionary rinds. They noted the differences in clast population of 72215 (and other Boulder 1 samples) from those of the coarser poikilitic melt breccias from the site.

CHEMISTRY

Chemical analyses of bulk melt matrix are reproduced in Table 3, arranged according to sampling domain and description. Rare earths for these analyses are plotted in Fig. 7. Analyses of the poikilitic feldspathic granulite (= anorthositic gabbro, poikilitic ANT breccia, lithology GA, domain 6, and class 4) are reproduced in Table 4, with the rare earths plotted in Fig. 8. Table 4 also reproduces a partial analysis of an "anorthositic" clast separated from a different area.

Table 3 and Fig. 7 show that all the different colored/textured matrix domains have essentially the same composition, The major elements are in substantial agreement with the compositions determined by microprobe defocused beam analyses (Table 1), except that the latter have slightly lower alumina. Two partial analyses of darker

Table 3: Chemical analyses of matrices/bulk rock samples of 72215.

	Slab; average matrix (ordinary breccia OB) Domains 2,3							Slab; dark sugary matrix (DSG) Dom 1			
	,64	,40	,22	,39a	,39b	,68a	,68b	,60	,59	,54	
Split wt %											Split wt.%
SiO_2	45.1		46.7					44.9			SiO_2
TiO_2	1.0		0.70					0.9			TiO_2
Al_2O_3	20.7		20.3					21.2			Al_2O_3
Cr_2O_3	0.265		0.243					0.25			Cr_2O_3
FeO	(a) 8.45		10.3					(b) 8.49			FeO
MnO	0.133		0.117					0.12			MnO
MgO	9.81		10.3					11.5			MgO
CaO	12.0		12.5					11.9			CaO
Na_2O	0.500		0.475					0.524			Na_2O
K_2O	0.323		0.214					0.235			K_2O
P_2O_5			0.236								P_2O_5
ppm											ppm
Sc	18.9		18.5					18.4			Sc
V											V
Co	23.8		26.9					29.5			Co
Ni	120	154	170					120	158		Ni
Rb		4.88							6.65	5.02	Rb
Sr			160							139.1	Sr
Y			90								Y
Zr			360								Zr
Nb			25								Nb
Hf	9.4		9.11					9.9			Hf
Ba			299								Ba
Th	4.5		3.94	4.298	3.768	4.656	4.327	5.5			Th
U		1.36	1.16	1.185	1.023	1.272	1.179		1.520		U
Cs			0.180						0.216		Cs
Ta	1.4		1.14					1.4			Ta
Pb				2.387	2.122	2.658	2.344				Pb
La	28		28.1					30			La
Ce	73		72.0					81			Ce
Pr											Pr
Nd			45								Nd
Sm	13.0		11.2					14.5			Sm
Eu	1.34		1.34					1.41			Eu
Gd			15.5								Gd
Tb	2.3		2.47					2.6			Tb
Dy			17.2								Dy
Ho			3.77								Ho
Er											Er
Tm			1.56								Tm
Yb	9.6		9.29					10.7			Yb
Lu	1.32		1.26					1.45			Lu
Li			12.2								Li
Be											Be
B											B
C											C
N											N
S			320								S
F			18.8								F
Cl			14.0								Cl
Br		0.0281	0.05						0.0286		Br
Cu											Cu
Zn		1.8							1.6		Zn
ppb											ppb
Au									2.26		Au
Ir									5.02		Ir
I											I
At											At
Ga			3900								Ga
Ge		141							144		Ge
As											As
Se		68							72		Se
Mo											Mo
Tc											Tc
Ru											Ru
Rh											Rh
Pd											Pd
Ag		0.461							0.464		Ag
Cd		3.6							3.0		Cd
In											In
Sn											Sn
Sb		0.66							0.92		Sb
Te		3.32							2.5		Te
W											W
Re		0.372							0.380		Re
Os											Os
Pt											Pt
Hg											Hg
Tl		0.53							0.63		Tl
Bi		0.14							0.32		Bi
	(1)	(2)	(3)	(4)	(4)	(4)	(4)	(1)	(2)	(5)	

References and methods:
(1) Blanchard et al. (1974); AAS, INAA
(2) Higuchi and Morgan (1975a), Morgan et al. (1975), Hertogen et al. (1977); RNAA
(3) Palme et al. (1978); XRF, MFB, INAA, RNAA
(4) Nunes and Tatsumoto (1975); IDMS
(5) Compston et al. (1975); XRF, IDMS
(6) Jovanovic and Reed (1974, 1975a,b,c,d, 1980); INAA

Notes:
(a) AAS; INAA = 8.45%
(b) AAS; INAA = 8.25%
(c) AAS; INAA = 8.57%
(d) AAS: INAA = 8.19%
(e) Poor Th concentration data.
(f) Combined leach and residue fractions.

Table 3: Continued

	Slab; dark sugary breccia (DSG)			Slab; light gray breccia (LB)					Knob; gray breccia		
	,61	,51a	,51b	,47	,44	,15a	,15b-1	,15b-2	,92	,88	
Split wt %											**Split wt %**
SiO_2				45.1					45.6		SiO_2
TiO_2				0.7					0.8		TiO_2
Al_2O_3				21.4					20.9		Al_2O_3
Cr_2O_3				0.251					0.224		Cr_2O_3
FeO				(c) 8.35					(d) 8.44		FeO
MnO				0.129					0.125		MnO
MgO				11.3					10.1		MgO
CaO				12.0					12.3		CaO
Na_2O				0.548					0.504		Na_2O
K_2O				0.195					0.253		K_2O
P_2O_5											P_2O_5
ppm											**ppm**
Sc				18.5					18.5		Sc
V											V
Co				31.6					23.0		Co
Ni				250	146				140	136	Ni
Rb					2.83					3.88	Rb
Sr											Sr
Y											Y
Zr											Zr
Nb											Nb
Hf				9.9					9.4		Hf
Ba											Ba
Th		4.871	4.635	4.8		(e) 4.633	(e) 4.081	5.084	3.1		Th
U		1.315	1.290		1.32	1.408	1.232	1.369		1.62	U
Cs					0.115					0.198	Cs
Ta				1.4					1.3		Ta
Pb		2.936				2.987	2.464	2.716			Pb
La				30					30		La
Ce				76					79		Ce
Pr											Pr
Nd											Nd
Sm				15.0					15.4		Sm
Eu				1.44					1.34		Eu
Gd											Gd
Tb				2.7					2.6		Tb
Dy											Dy
Ho											Ho
Er											Er
Tm											Tm
Yb				11.1					9.9		Yb
Lu				1.47					1.25		Lu
Li											Li
Be											Be
B											B
C											C
N											N
S											S
P											P
Cl											Cl
Br					0.0222					0.0344	Br
Cu											Cu
Zn					1.7					1.8	Zn
ppb											**ppb**
Au					2.06					1.76	Au
Ir					5.34					3.92	Ir
I											I
At											At
Ga											Ga
Ge					117					124	Ge
As											As
Se					49					71	Se
Mo											Mo
Tc											Tc
Ru	8										Ru
Rh											Rh
Pd											Pd
Ag					0.562					0.466	Ag
Cd					3.8					5.3	Cd
In											In
Sn											Sn
Sb					0.64					0.71	Sb
Te					2.4					4.9	Te
W											W
Re					0.397					0.279	Re
Os	21										Os
Pt											Pt
Hg											Hg
Tl					0.41					0.46	Tl
Bi					0.29					0.45	Bi
	(6)	(4)	(4)	(1)	(2)	(4)	(4)	(4)	(1)	(2)	

Table 3: Continued

	Knob; dark sugary breccia			
	,100	,104 gray	,104 dk a	,104 dk b
Split wt %				
SiO_2				
TiO_2				
Al_2O_3				
Cr_2O_3				
FeO				
MnO				
MgO				
CaO				
Na_2O				
K_2O				
P_2O_5	0.57			
ppm				
Sc				
V				
Co				
Ni				
Rb		4.05	44.19	43.98
Sr		149.7	162.2	161.0
Y				
Zr				
Nb				
Hf				
Ba				
Th				
U	3.1			
Cs				
Ta				
Pb				
La				
Ce				
Pr				
Nd				
Sm				
Eu				
Gd				
Tb				
Dy				
Ho				
Er				
Tm				
Yb				
Lu				
Li	11			
Be				
B				
C				
N				
S				
F	129			
Cl	(f) 58.8			
Br	(f) 0.732			
Cu				
Zn				
ppb				
Au				
Ir				
I	1.1			
At				
Ga				
Ge				
As				
Se				
Mo				
Tc				
Ru				
Rh				
Pd				
Ag				
Cd				
In				
Sn				
Sb				
Te				
W				
Re				
Os				
Pt				
Hg				
Tl				
Bi				
	(6)	(5)	(5)	(5)

material picked from 72215,104, from the knob area, differ in having extremely high Rb. Possibly these represent domain 5. The melt matrix compositions are similar to those of petrographically similar materials from the other Boulder 1 samples. They are a low-K Fra Mauro composition, (K20 -0.2 - 0.3%), and differ from the coarser poikilitic melts at the site in being slightly more aluminous and less titaniferous. The siderophile element ratios are also distinct from those of these coarser melts; Morgan et al. (1975) placed 72215 along with other Boulder 1 samples in a meteoritic Group 3L, distinct from the common Group 2 at Apollo 17. However, Blanchard et al. (1974, 1975) and Winzer et al. (1975) emphasize the similarity of all the melts at the Apollo 17 site.

The data of Jovanovic and Reed (several publications; see Table 1) include analyses for leach and residue fractions for some elements; these are combined for Table 1. They discuss some of their data as suggesting vapor clouds being responsible for the leachable materials, and with varied parents for the non-leachable materials.

RADIOGENIC ISOTOPES

Schaeffer et al. (1982a,b) used laser Ar-Ar techniques to determine ages of clasts and to infer the age of the melt in section 72215,144, providing 16 analyses (Table 5). Most of the ages were for plagioclase and felsite ("feldsparthoid") clasts. The felsite clasts give the youngest ages, averaging 3.83 Ga; the higher ages for the plagioclases range up to 4.02 Ga; some of these plagioclases are in noritic lithic clasts. The age of the felsite clasts, which probably degassed during melting, is the best estimate for the age of the melt groundmass, which is therefore about 3.83 Ga old. (The felsite clasts were preheated to 650 degrees C. The ages are total release, hence K-Ar, of the greater than 650

Table 4: Chemical analyses of poikilitic feldspathic granulate and other anorthositic materials in 72215.

	Domain 6 (Cumulate)				
	,76	,89	,102	,54	
Split	wt %				wt %
SiO_2	44.7				SiO_2
TiO_2	0.5				TiO_2
Al_2O_3	27.3				Al_2O_3
Cr_2O_3	0.126				Cr_2O_3
FeO	(a) 4.80				FeO
MnO	0.067				MnO
MgO	7.19				MgO
CaO	14.9				CaO
Na_2O	0.483				Na_2O
K_2O	0.113				K_2O
P_2O_5			0.12		P_2O_5
ppm					ppm
Sc	7.68				Sc
V					V
Co	11.9				Co
Ni	50	56			Ni
Rb		1.44		0.82	Rb
Sr				164.6	Sr
Y					Y
Zr					Zr
Nb					Nb
Hf	2.4				Hf
Ba					Ba
Th	1.30				Th
U		0.0516		0.16	U
Cs					Cs
Ta	0.310				Ta
Pb					Pb
La	7.3				La
Ce	18.3				Ce
Pr					Pr
Nd					Nd
Sm	3.36				Sm
Eu	1.00				Eu
Gd					Gd
Tb	0.66				Tb
Dy					Dy
Ho					Ho
Er					Er
Tm					Tm
Yb	3.1				Yb
Lu	0.44				Lu
Li			9.2		Li
Be					Be
B					B
C					C
N					N
S					S
F					F
Cl		(b) 0.0290	(b) 0.052		Cl
Br					Br
Cu		1.3			Cu
Zn					Zn
ppb					ppb
Au		0.013			Au
Ir		2.95			Ir
I					I
At					At
Ga					Ga
Ge		2.2			Ge
As					As
Se					Se
Mo					Mo
Tc					Tc
Ru					Ru
Rh					Rh
Pd					Pd
Ag		0.502			Ag
Cd		6.7			Cd
In					In
Sn					Sn
Sb		0.31			Sb
Te		15.4			Te
W					W
Re					Re
Os					Os
Pt					Pt
Hg					Hg
Tl		0.59			Tl
Bi		<0.71			Bi
	(1)	(2)	(3)	(4)	

References:
(1) Blanchard et al. (1974); AAS, INAA
(2) Higuchi and Morgan (1975a), Morgan et al. (1975), Hertogen et al. (1977); RNAA
(3) Jovanovic and Reed (1974, 1975a,b,c,d,1980); INAA
(4) Compston et al. (1975); IDMS

Notes:
(a) AAS; INAA = 4.59%
(b) Combined residue and leach fractions

Compston et al. (1975) reported Rb-Sr isotopic data for whole-rock samples of matrix and an "anorthosite" clast in 72215 (Table 6). The matrix and anorthosite clast fall on a mixing line of about 4.4 Ga, and the Sr isotopes did not equilibrate on the scale of the plagioclase crystals (< 0.1mm). Thus the time for high-temperature assembly was very short. The dark gray matrix fraction has a high Rb content that presumably reflects micro-granite. This fraction forms a precise 3.95 +/-0.03 Ga alignment with the anorthosite-depleted matrix fractions and BABI (Fig. 9); this age is a well-determined age for the granites, and is not sensitive to even quite large errors in estimating the Rb/Sr ratio of the granite. These granites are older than the breccia-forming event.

Nunes and Tatsumoto (1975) reported U, Th, Pb isotopic data for 6 matrix samples of 72215, deriving some age parameters (reproduced as Tables 7a,b,c). The data are shown, with other samples from Boulder 1, on Fig. 10, a lead concordia diagram. All data, corrected for blanks and assumed primordial Pb, lie within estimated uncertainty of a 3.94.4 Ga discordia line, typical of many lunar highlands rocks. Nunes and Tatsumoto (1975) interpret the 4:4 Ga intersection as merely representing an average of events older and younger than 4.4 Ga, and the 3.9 Ga intersection representing differentiation or metamorphic events at that time. Braddy et al. (1975) reported that they measured P and U fission tracks in whitlockites and zircons in 72215, but presented no data or results. They found zircons large enough to date in sections.

degrees C fraction. Assuming there is a well-developed plateau above that temperature, the ages are reliable).

Compston et al. (1975) reported Rb-Sr isotopic data for whole-rock samples of matrix and an "anorthosite" clast in 72215 (Table 6). The matrix and anorthosite clast fall on a mixing line of about 4.4 Ga, and the Sr isotopes did not equilibrate on the scale of the plagioclase crystals (< 0.1mm). Thus the time for high-temperature assembly was very short. The dark gray matrix fraction has a high Rb content that presumably reflects micro-granite. This fraction forms a precise 3.95 +/-0.03 Ga alignment with the anorthosite-depleted matrix fractions and BABI (Fig. 9); this age is a well-determined age for the granites, and is not sensitive to even quite large errors in estimating the Rb/Sr ratio of the granite. These granites are older than the breccia-forming event.

Nunes and Tatsumoto (1975) reported U, Th, Pb isotopic data for 6 matrix samples of 72215, deriving some age parameters (reproduced as Tables 7a,b,c). The data are shown, with other samples from Boulder 1, on Fig. 10, a lead concordia diagram. All data, corrected for blanks and assumed primordial Pb, lie within estimated uncertainty of a 3.94.4 Ga discordia line, typical of many lunar highlands rocks. Nunes and Tatsumoto (1975) interpret the 4:4 Ga intersection as merely representing an average of events older and younger than 4.4 Ga, and the 3.9 Ga intersection representing differentiation or metamorphic events at that time. Braddy et al. (1975) reported that they measured P and U fission tracks in whitlockites and zircons in 72215, but presented no data or results. They found zircons large enough to date in sections.

Table 5: Laser microprobe data for materials in 72215,144.
Recalculated from Schaeffer *et al.* (1982a,b).

Phase	K%	Ca%	Ar40/39	Age Ga
K-spar*	3.1	2	35.85+/-0.49	3.905 +/-.040
Plag	0.27	3	35.68 0.72	3.847 .039
Plag	1.2	6	36.82 0.34	3.897 .027
Plag	0.05	1	38.06 0.88	3.949 .044
Plag	0.10	1	39.85 0.91	4.022 .043
Plag	0.14	6	36.14 2.26	3.867 .103
Plag/comp	0.07	1	36.56 0.61	3.885 .035
Pyroxene	0.03	2	30.49 1.17	3.602 .064
Matrix	0.12	2	32.98 0.33	3.723 .027
Felsite*	6	<10	34.66 0.99	3.847 .042
Felsite*	6	<10	31.10 0.75	3.682 .050
Felsite*	9	<10	35.03 0.60	3.868 .043
Felsite*	3	<10	35.40 1.80	3.885 .088
Felsite*	3	<10	33.77 1.30	3.810 .070
Felsite*	8	<10	34.29 0.55	3.835 .041
Felsite*	5	<10	35.76 0.80	3.899 .050

(Samples degassed at 225 degrees centigrade during bakeout after sample loading)
* = preheated at 650 degrees centigrade

Table 6: Rb-Sr isotopic data for samples from 72215
(Compston *el al*., 1975).

Sample	Mass mg	Rb ppm	Sr ppm	87Rb/86Sr	87Sr/86Sr
,54 gray	12.0	5.02	139.1	0.1042	0.70572+/-3
,54 anorth	11.2	0.86	164.6	0.01514	0.70006 2
,104 gray	15.8	4.05	149.7	0.0782	0.70424 3
,104 dark gray A	14.7	44.19	162.2	0.7893	0.74534 3
,104 dark gray B	13.9	43.98	161.0	0.7915	0.74513 4

Table 7a: Concentrations of U, Th, and Pb in 72215 samples
(Nunes and Tatsumoto, 1975).

Concentrations of U, Th, and Pb in some Apollo 17 whole-rock samples from Boulder 1

Sample	Description	Run	Weight (mg)	Concentrations			$^{232}Th/^{238}U$	$^{238}U/^{204}Pb$
				U	Th	Pb		
72215,15	Dark clast (GCBx)	C1	46.1	1.408	(4.633)	2.987	(3.40)	2801
72215,15	Light-gray breccia (GCBx)	C1	46.0	1.232	(4.081)	2.464	(3.42)	3227
		C2[a]	85.5	1.369	5.084	2.716	3.84	1890
72215,51	Sugary dark gray breccia (GCBx)	C1	48.8	1.316	4.871	2.936	3.82	2069
		C2[a]	98.1	1.290	4.635	[b]	3.71	[b]
72215,68	Ordinary breccia (GCBx)	C1	55.0	1.272	4.656	2.658	3.78	1010
		C2[a]	101.8	1.179	4.327	2.344	3.79	2480
72215,39	Ordinary breccia (GCBx)	C1	47.1	1.185	4.298	2.387	3.75	7353
72215,39	Light-gray breccia (GCBx)	C1	41.3	1.023	3.768	2.122	3.81	3322
72275,170	Pigeonite basalt clast (PB)	C1	38.6	1.635	6.255	3.047	3.95	3045

[a] Totally spiked sample data; other data were spiked after solution aliquoting.
[b] Underspiking and uncertainty in the sample $^{208}Pb/^{206}Pb$ yielded poor Pb concentration data.
Data in parentheses uncertain owing to poor Th concentration data.
All 72215 samples are competent breccias with colors ranging from black to light-gray.
C=concentration run (GCBx)=gray competent breccia (PB)=pigeonite basalt.

Table 7b: Isotopic composition of Pb in 72215 samples
(Nunes and Tatsumoto, 1975).

Isotopic composition of Pb in some Apollo 17 whole-rock samples from Boulder 1

Sample	Description	Run	Weight (mg)	Observed Ratios[c]		Corrected for Analytical Blank[b]					
				$^{206}Pb/^{204}Pb$	$^{207}Pb/^{204}Pb$	$^{208}Pb/^{204}Pb$	$^{206}Pb/^{204}Pb$	$^{207}Pb/^{204}Pb$	$^{208}Pb/^{204}Pb$	$^{207}Pb/^{206}Pb$	$^{208}Pb/^{206}Pb$
72215,15	Dark clast (GCBx)	P	49.8	1402	786.6	1363	4491	2508	4323	0.5584	0.9625
		C1	46.1	1118	628.7	–	2730	1528	–	0.5596	–
72215,15	Light-gray breccia (GCBx)	P	48.5	1593	837.3	1545	(36540)	(19073)	(34980)	0.5220	0.9573
		C1	46.0	1040	549.3	–	3016	1581	–	0.5226	–
		C2[a]	85.5	1382	714.6	–	1755	906.1	–	0.5162	–
72215,51	Sugary dark gray breccia (GCBx)	P	47.3	505.7	293.2	498.1	686.0	396.0	668.4	0.5772	0.9744
		C1	48.8	1010	580.1	–	2094	1198	–	0.5720	–
		C2[a]	98.1	1059	627.6	–	1219	721.6	–	0.5920	–
72215,68	Ordinary breccia (GCBx)	P	37.2	933.0	514.2	902.2	2899	1586	2759	0.5471	0.9520
		C1	55.0	662.9	366.9	–	979.1	539.3	–	0.5508	–
		C2[a]	101.8	1716	891.5	–	2311	1199	–	0.5186	–
72215,39	Ordinary breccia (GCBx)	P	38.3	1207	635.2	1180	3952	2066	3815	0.5227	0.9656
		C1	47.1	1629	855.5	–	6892	3599	–	0.5223	–
72215,39	Light-gray breccia (GCBx)	P	39.0	1383	763.3	1332	(11731)	(6432)	(11145)	0.5483	0.9500
		C1	41.3	1096	605.3	–	3197	1756	–	0.5492	–
72275,170	Pigeonite basalt clast (PB)	P	38.9	2360	1079	2387	(34287)	(15592)	(34420)	0.4547	1.0038
		C1	38.6	1299	597.2	–	2672	1220	–	0.4568	–

P=composition run; C=concentration run; (GCBx)=gray competent breccia; (PB)=pigeonite basalt.
[a] Totally spiked runs from solid sample splits; other runs were obtained from samples which were divided from solution.
[b] Pb blanks ranged from 1.4 to 2.1 ng for the solution aliquoted data and were 1.05 ng for the totally spiked data.
[c] Raw data corrected for mass discrimination of 0.15% per mass unit. ^{208}Pb spike contribution subtracted from concentration data.
Data in parentheses subject to extreme error owing to Pb blank uncertainty.
All 72215 samples are competent breccias with colors ranging from black to light-gray.

P. D. NUNES AND M. TATSUMOTO

Table 7c: Age parameters and single-stage ages for 72215 samples
(Nunes and Tatsumoto, 1975).

Age parameters and single-stage ages of some Apollo 17 Boulder 1 whole-rock samples

Sample	Description	Run	Atomic ratios corrected for blank and primordial Pb				Single-stage ages × 10^6 yr			
			$\frac{^{206}Pb}{^{238}U}$	$\frac{^{207}Pb}{^{235}U}$	$\frac{^{207}Pb}{^{206}Pb}$	$\frac{^{208}Pb}{^{232}Th}$	$\frac{^{206}Pb}{^{238}U}$	$\frac{^{207}Pb}{^{235}U}$	$\frac{^{207}Pb}{^{206}Pb}$	$\frac{^{208}Pb}{^{232}Th}$
72215,15	Dark clast (GCBx)	C1P	0.9726	74.73	0.5573	0.2740	4380	4394	4400	4895
		C1	0.9713	74.70	0.5577	–	4375	4393	4402	–
72215,15	Light-gray breccia (GCBx)	C1P	0.9344	67.23	0.5218	0.2612	4253	4288	4304	4690
		C1	0.9317	67.13	0.5226	–	4244	4286	4306	–
		C2[a]	0.9299	66.36	0.5131	–	4218	4259	4279	–
72215,51	Sugary dark gray breccia (GCBx)	C1P	0.9985	78.47	0.5699	0.2466	4464	4443	4433	4455
		C1	1.008	79.14	0.5696	–	4493	4451	4432	–
72215,68	Ordinary breccia (GCBx)	C1P	0.9657	72.61	0.5453	0.2421	4357	4365	4368	4367
		C1	0.9596	72.17	0.5455	–	4337	4359	4369	–
		C2[a]	0.9286	66.09	0.5162	–	4234	4271	4288	–
72215,39	Ordinary breccia (GCBx)	C1P	0.9351	67.22	0.5214	0.2397	4256	4288	4303	4343
		C1	0.9360	67.30	0.5215	–	4259	4288	4303	–
72215,39	Light-gray breccia (GCBx)	C1P	0.9616	72.64	0.5479	0.2395	4343	4365	4375	4340
		C1	0.9596	72.49	0.5476	–	4337	4363	4375	–
72275,170	Pigeonite basalt clast (PB)	C1P	0.8776	55.00	0.4547	0.2228	4061	4087	4100	4065
		C1	0.8747	54.82	0.4545	–	4051	4084	4100	–

[a] Concentrations determined from totally spiking a separate sample. Concentration and composition splits were divided from perfect solutions prior to spiking for all other analyses.
All 72215 samples are competent breccias with colors ranging from black to light-gray.
P=composition run; C=concentration run; (GCBx)=gray competent breccia; (PB)=pigeonite basalt.

U–Th–Pb SYSTEMATICS OF SELECTED SAMPLES FROM APOLLO 17, BOULDER 1, STATION 2

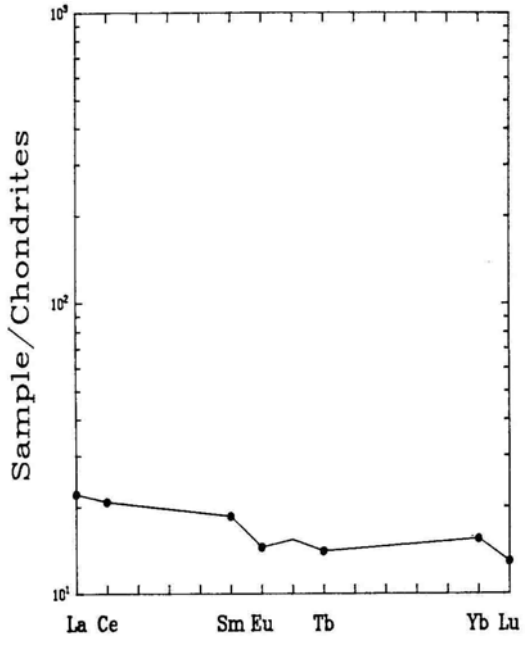

Figure 8: Rare earth element plot for poikilitic feldspathic granulite in 72215. Blanchard et al (1975).

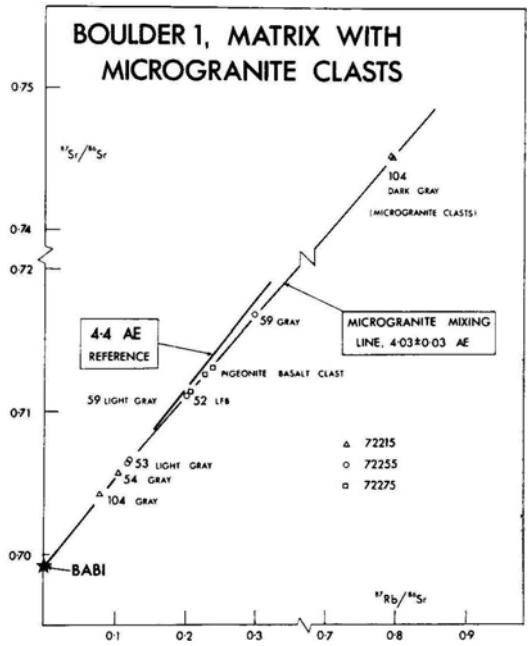

Figure 9: Mixing line defined by 72215,104 dark gray and other samples. The mixing line determines the age of the micro-granite, which dominates 72215,104 dark gray, because the micro-granites are so radiogenic. The 4.03 Ga age is calculated using the "old" Rb decay constants; using the constant of 1.42 x 10-^{11}1yr gives 3.95 Ga.

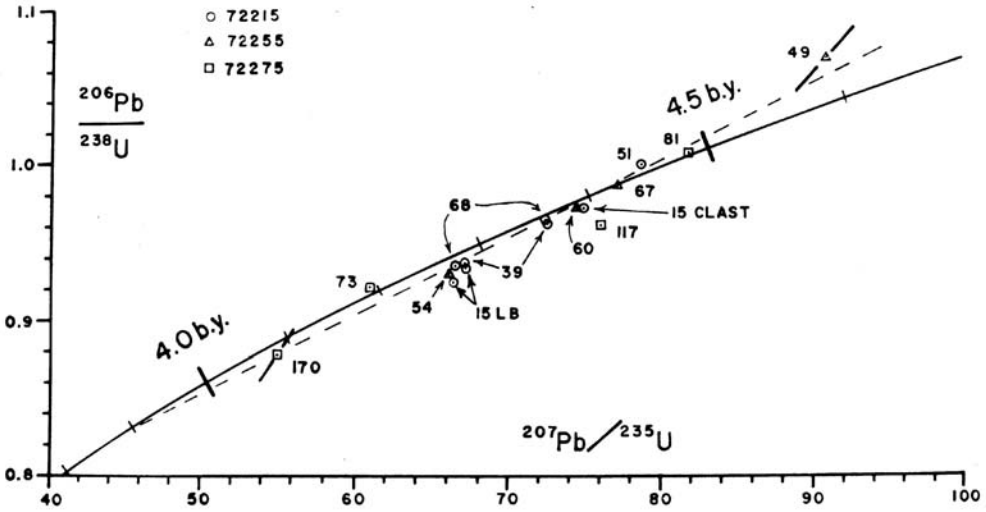

Concordia diagram (Wetherill, 1956) with Boulder 1 data corrected for blanks and primordial Pb. All data for 72215 (circles) and pigeonite basalt clast 72275,170 are from this report; all other 72275 (squares) and 72255 (triangles) data are from Nunes *et al.* (1974a). U/Pb errors of ±2% are shown for the two most extreme analyses, but are omitted from the other data points for clarity. Individual analyses are labelled with their subnumbers. LB=light-gray breccia; b.y.=10^9 yr. Anorthositic breccia clast 72275,117 is considered to lie outside of error below the 3.9–4.4 b.y. discordia line; all other samples, including matrix sample 72275,73, lie within error of this line.

Figure 10. Concordia diagram for 72215 and other Boulder I samples (Nunes and Tatsumoto, 1975).

EXPOSURE AGES

Leich et al. (1975) measured the isotopic compositions of the rare gases He, Ne, Ar, Kr, and Xe in three matrix samples from 72215. Trapped gas abundances are very low, with only small to negligible solar wind components. The cosmogenic Kr isotopic spectra give an exposure age of 41.4 +/-1.4 Ma, in good agreement with that of 72255. It is lower than the exposure age of 72275 (52 Ma), probably because of differences in shielding.

PHYSICAL PROPERTIES

Magnetic data for 72215 samples were reported by Banerjee and Swits (1975) and Banerjee and Mellema (1976 a,b,c), with the aim of determining paleointensity (Table 8). The average direction of NRM was the same as that in 72255 and 72275,while the stable components differed in direction.

The Shaw method suggests an averaged large field of 0.41 Oe at 4.0 Ga at Taurus-Littrow. This is similar to the size of the field determined from carbonaceous chondrites; the authors suggest a field of solar origin. Cisowski et al. (1977) noted that 72215 did not have hysteresis characterization available, and did not have the minimal requirements of a single phase NRM. Thus, they did not accept the paleointensity measurement as meaningful.

Adams and Charette (1975) and Charette and Adams (1977) obtained reflectance spectra for chips and powders of 72215 (Fig. 11). All the samples have absorption bands near 0.9 and 1.9 microns, from Fe^{2+} in orthopyroxene. The anorthositic gabbro curve (poikilitic feldspathic granulite), 72215,101, is characterized by deep pyroxene and plagioclase Fe^{2+} bands; a high left shoulder at 0.7 microns relative to right shoulder at 1.1 microns; and the absence of any absorption feature near 0.6 microns. The lighter breccias differ from the darker ones, with the latter (,58) having weaker pyroxene and plagioclase bands, more-nearly equal shoulders, and a flatter slope of the continuum.

PROCESSING

The details of the processing of 72215 were given by Marvin in Cl 2 (1974), with detailed allocation information. During PET in 1973 a documented chip was used for thin sections, and others were later taken for varied purposes. Marvin and Agrell made detailed surface maps (July 1973). A single saw cut was planned to section all features of interest across the foliation; during sawing (1974) the knob broke from the main slab, producing several subsamples (Fig. 2). Two thin subslabs were cut through the original slab, and devoted to thin sections (Fig. 12).

Table 8: Paleointensity determinations for 72215 samples (Banerjee and Mellema, 1976)

Sample #	Number of determinations	H (Oersted)	s.d	Range (Oersted)
,56	7	0.55	0.10	0.74-0.44
,46	7	0.41	0.17	0.60-0.21
,93	8	0.28	0.07	0.37-0.18

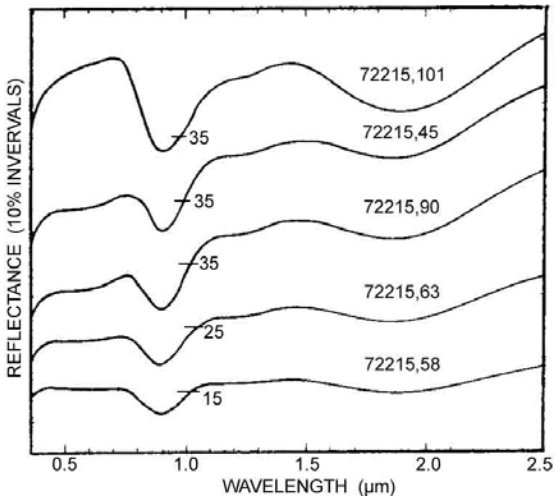

Figure 11: Spectral reflectance diagrams for 72215 samples (Adams and Charette, 1975). 101 is poikilitic feldspathic granulite (anorthositic gabbro);,45 and,90 are light to medium-gray matrix; ,58 is dark matrix; and,63 is matrix intermediate to dark and light.

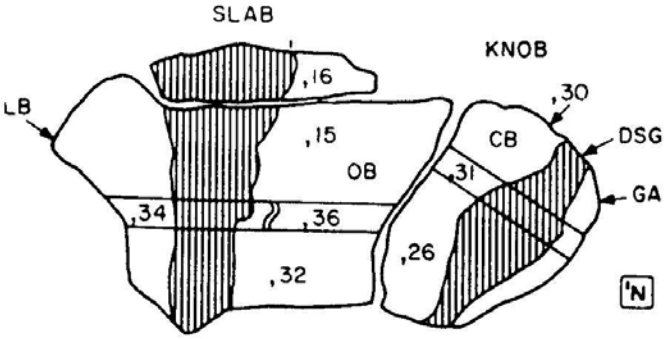

Figure 12: Dissection of the original slab to show the source of the thin section transect (,31; ,36; ,34) and other sample numbers (from Marvin, C12,1974).